Stabilization of a Three-Dimensional Limit Cycle Walking Model through Step-to-Step Ankle Control

Myunghee Kim and Steven H. Collins
Department of Mechanical Engineering
Carnegie Mellon University, Pittsburgh, Pennsylvania 15213-3815
biomechatronics.cit.cmu.edu, myunghek@cmu.edu

***Abstract*—Unilateral, below-knee amputation is associated with an increased risk of falls, which may be partially related to a loss of active ankle control. If ankle control can contribute significantly to maintaining balance, even in the presence of active foot placement, this might provide an opportunity to improve balance using robotic ankle-foot prostheses. We investigated ankle- and hip-based walking stabilization methods in a three-dimensional model of human gait that included ankle plantar-flexion, ankle inversion-eversion, hip flexion-extension, and hip ad/abduction. We generated discrete feedback control laws (linear quadratic regulators) that altered nominal actuation parameters once per step. We used ankle push-off, lateral ankle stiffness and damping, fore-aft foot placement, lateral foot placement, or all of these as control inputs. We modeled environmental disturbances as random, bounded, unexpected changes in floor height, and defined balance performance as the maximum allowable disturbance value for which the model walked 500 steps without falling. Nominal walking motions were unstable, but were stabilized by all of the step-to-step control laws we tested. Surprisingly, step-by-step modulation of ankle push-off alone led to better balance performance (3.2% leg length) than lateral foot placement (1.2% leg length) for these control laws. These results suggest that appropriate control of robotic ankle-foot prosthesis push-off could make balancing during walking easier for individuals with amputation.**

I. Introduction

Individuals with unilateral below-knee amputation experience a higher risk of falls and fear of falling [1]. This may be related to reduced balance ability, in part due to lost sensing and actuation capabilities at the ankle joint. Robotic ankle-foot prostheses, whose improved actuation has recently been shown to reduce energy cost [2], might also restore ankle control related to balance and reduced fall risk. However, the relative contribution of ankle control to overall balance remains unclear.

Hip control associated with foot placement and ankle control associated with center of pressure adjustment seem to be important for balance during walking. Foot placement can have a large impact on mechanical work during step-to-step transitions [3], with relatively little energy consumed through hip actuation [4], allowing recovery from large disturbances [5]. When the foot is flat on the ground, ankle torques allow direct control of the center of pressure [6], an effect central to the control of many successful humanoid robots [e.g. 7]. Unfortunately, ankle-foot prostheses cannot directly control foot placement and have very limited capacity to control center of pressure progression in under-actuated human gait.

Step-by-step control of ankle push-off work has also been suggested as a means of stabilizing locomotion. Push-off work, performed by ankle plantarflexion during the latter portion of the stance period, has a strong effect on system energy following double support [8]. Increasing or decreasing this push-off based on state feedback once per step can be an effective means of stabilizing two-dimensional walking robots [9], particularly when used in combination with foot placement [10]. Step-by-step control of ankle push-off might be suitable for use in robotic ankle-foot prostheses, since active push-off appears to be an important function for such devices [2]. The effects of push-off modulation in three-dimensional walking systems have not yet been studied, however, and their importance relative to foot placement and center of pressure control are not well understood.

Limit cycle models of walking have been used extensively to study gait dynamics and stability in simulation, and may provide a useful means of comparing candidate prosthesis control techniques. Basic models of this type have provided insights into fundamental aspects of human walking, such as the relationship between ankle push-off work and energy use [11] or between crouch gait and stiff-knee gait [12]. Similar models suggest that lateral motions in human gait are passively unstable, but can be stabilized through active control of step-width or ankle inversion-eversion torques [4], a finding corroborated by experimental work [13, 14]. Similar models could allow for exploration of the role of active prosthesis control in overall walking balance for individuals with amputation. Successful control designs could then be embedded in prosthesis hardware, as with limit-cycle based walking robots [10, 15–17].

The purpose of this study was to investigate the effectiveness of step-by-step ankle push-off control for stabilizing gait and to compare its utility to foot placement and limited center of pressure control. We developed a three-dimensional limit-cycle model of amputee locomotion with ankle and hip actuation. External disturbances were applied in the form of a series of random floor height changes. We designed high-level controllers that discretely modulated actuation parameters at each step, including ankle push-off, inversion-eversion resistance, and foot placement. We then compared the maximum allowable disturbance for each controller.

978-1-4673-6024-1/13/$31.00 ©2013 IEEE

II. Methods

We developed a three-dimensional model of walking with ankle and hip actuation to compare the stabilizing effects of different control strategies at these joints. The model was comprised of flat feet, straight legs, and a pevlvis. The feet connected to the legs via ankles allowing for plantar flexion and inversion, and the straight legs connected to the pelvis via hips, allowing for flexion and abduction. We developed nominal controllers for the hip and ankle and modulated their parameters once per step using a variety of strategies related to foot placement, lateral center of pressure modulation, and push-off work. We measured the stability performance of each step-to-step controller as the maximum random ground height that the model could tolerate without falling.

A. Three-Dimensional Limit Cycle Walking Model

The model had two legs without knees, feet, and a pelvis with finite width. We chose parameter values to approximate those of humans [18, 19], including: pelvis mass = 54 Kg, leg inertia = 10 Kg·m^2, leg mass = 10 Kg, leg length = 1 m, distance from leg center of mass to ankle = 0.7 m, ankle height = 0.09 m, horizontal distance between toe and ankle = 0.2 m, foot length = 0.25 m, foot width = 0.1 m, hip width = 0.3 m, and nominal step width = 0.15 m.

During each step, the model traveled through three continuous phases: double support, fully actuated single support, and under-actuated single support (Fig. 2). During fully actuated single support, the model had three actuted degrees of freedom: ankle plantarflexion, q_{ap}, ankle inversion, q_{ai}, and hip flexion, q_{hf}. During under-actuated single support, the model had the three actuated degress of freedom mentioned above, with the addition of a fourth degree of freedom: unactuated toe pitch, q_{tp}. During double support, the model had two degrees of freedom: one degree of freedom in the kinematic chain from trailing toe to leading ankle and one by allowing the trailing toe to 'slip' in yaw. Toe slipping was allowed during double support to avoid unrealistic kinematic coupling.

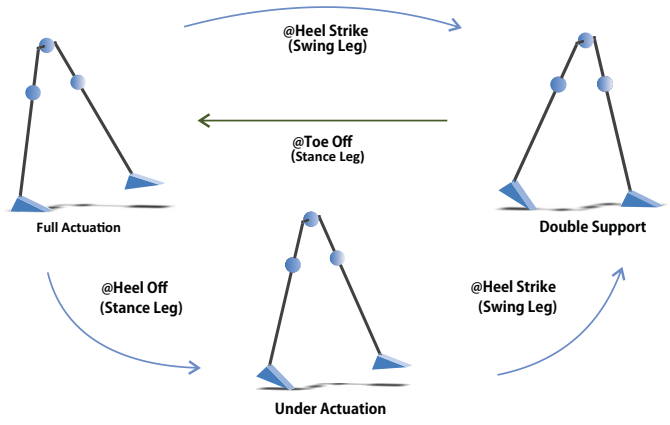

Fig. 1. Model gait phases. From the fully actuated single support phase, the model could transition either to double support or to under-actuated single support. Transitions were detected based on either heel strike of the swing foot or heel lift off of the stance foot. From double support, the model transitioned to fully actuated single support when the vertical component of force at the trailing toe became zero.

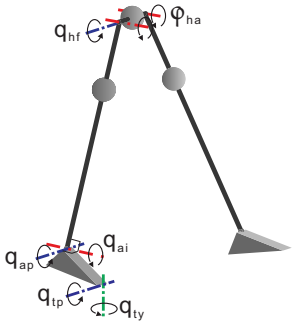

Fig. 2. Model degrees of freedom. The model comprised flat feet, straight legs, and a finite-width pelvis. During single support, the hip could rotate in flexion, q_{hf}, the ankle in plantarflexion, q_{ap}, and inversion-eversion, q_{ai}, and the toe was either fixed (during heel contact) or allowed to rotate in pitch, q_{tp}. Hip adduction-abduction angle, ϕ_{ha}, was instantaneously changed at the beginning of each step, then remained constant. During double support, the leading foot was fixed flat against the ground, and an additional degree of freedom in the trailing toe, q_{ty}, allowed rotational slipping about a vertical axis.

We obtained equations of motion for each phase using Kane's method [20]. State trajectories were obtained through numerical forward integration. Transitions between phases were detected based on heel lift off, heel strike, and toe lift off, as appropriate, and post-event states were calculated using angular momentum conservation about degrees of freedom for the post-event model, assuming perfectly inelastic collisions. We then found limit cycles by iteratively adjusting initial conditions using a gradient descent approach until the initial and final conditions matched.

B. Stability Metric

A measure of stability would ideally quantify the likelihood of falling under realistic circumstances. We considered several possible stability metrics for this application. Maximum Floquet multipliers apply to a linear region near the fixed point, which is often small and not characteristic of behavior under moderate disturbances [15]. The basin of attraction is difficult to calculate, and interpretation is made difficult because it does not capture rate of return or likelihood of being disturbed in a particular direction. The gait sensitivity norm [15] needs a well-chosen and validated gait indicator. Maximum allowable disturbance measures have greater utility, but do not account for consecutive disturbances. We used a stability measure which we propose is more directly related to the likelihood of falling under normal conditions: the maximum random floor height disturbance, applied once per step, which the model could tolerate without falling.

Random floor height changes capture aspects of real world disturbances such as random changes in floor conditions, sensory noise, and muscle actuation. Walking without falling under a higher random disturbance condition might show less likelihood of falling in the real world. Hence, we compared ankle actuation effects on stability to other step-to-step controllers by measuring maximum tolerable ground height disturbance while the model took five hundred steps. We decided the number of steps based on a simulation study. Fig. 4 shows the maximum tolerable random height depending on the number of steps. We generated five random terrain sets for each step. In Fig. 4, the dots represent the mean

of the five trials and they approached a constant. After five hundred steps, the error between the mean of the maximum tolerable height to the constant became less than 1%. The standard deviation for each trial, shown by the error bars, was less than 1% . Hence, we selected five hundred steps to measure maximum tolerable random height. Maximum Floquet multipliers, maximum single disturbance, and the gait sensitivity norm did not show a consistent relationship with the maximum allowable random height.

C. Actuation

The hip joints were actuated to obtain desired lateral and fore-aft foot placement, and the ankle joints were actuated to provide desired push-off work and inversion/eversion resistance. During each step, continuous low-level control was implemented, with nominal parameters corresponding to a limit cycle. Once per step, a high-level controller modulated hip and ankle control parameters to improve disturbance recovery.

We used proportional-derivative feedback control on hip flexion to achieve a target angle, ϕ_{hf}, with a nominal value corresponding to preferred step length for human walking (Fig. 5B). We tuned the gains of this controller to achieve critical damping and to ensure the swing leg reached the target angle by 90% of the gait cycle, similar to [21]. During each step, a constant hip abduction angle, ϕ_{ha}, was maintained, corresponding to preferred human step width. We applied low-gain proportional-derivative control on ankle inversion/eversion, with nominal values of zero for K_p and K_d. Ankle plantar-flexion torque was determined as a combination of a spring-like torque, with stiffness K, and a velocity-dependent offset, with magnitude τ_p. Nominal values of these parameters were chosen to roughly approximate the behavior of the human ankle during walking. Using these nominal actuation parameters, we used a gradient descent method to find a limit cycle with a walking speed of 1.25 m·s^{-1} and step length of 0.7 m.

Once a step, the high-level controller modulated the actuation parameters of the low-level controller. The high-level controller took the state after one step as an input, and generated new nominal actuation parameters for the next step. We linearized the step-to-step dynamics to obtain model

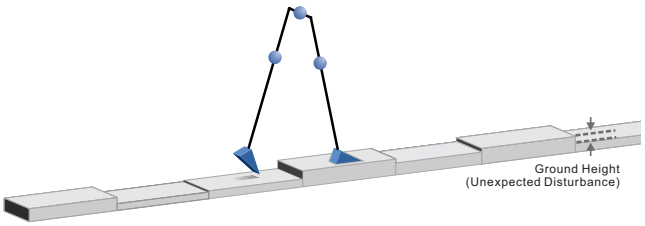

Fig. 3. Ground height disturbance modeling. The ground was modeled as a series of flat surfaces, centered on the foot at heel strike, in which height was varied as a random, bounded distribution. Magnitude of this disturbance was defined as the maximum possible difference between the height on two subsequent steps. Stability was characterized as the maximum disturbance magnitude for which the model walked 500 steps without falling.

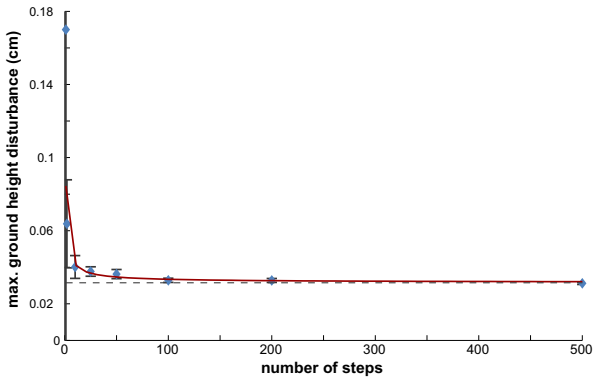

Fig. 4. The relationship between maximum allowable random floor height disturbance and the number of steps tested. Blue dots are the mean of five tests of maximum allowable disturbance using different randomized height patterns. Error bars are the standard deviation of the five trials. As the number of steps increased, the mean approached a constant value and the standard deviation decreased. We fit an exponential curve to this data, and found maximum disturbance $\approx 0.0315 + 0.0529 * (numsteps)^{(-0.7215)}$.

and control authority matrices, and then we used these to generate a linear quadratic regulator for high-level control. We tuned the output and input weight matrices to try to improve performance. The control sequence was as follows: 1) The model took one walking step. 2) At a predefined event, such as mid-stance or heel strike, the system state was measured. 3) The controller calculated the error by subtracting the measured state from the fixed-point state. 4) New low-level actuation parameters were calculated as the nominal parameter values plus the multiplication of the error with the control gain matrix. 5) The model took another step using the new actuation parameters.

We made high-level foot placement control decisions at mid-stance, and high-level ankle control decisions following heel strike. For foot placement, mid-stance appears to be a good moment to take a poincaré section [10] because the lateral velocity and displacement of the center of mass are well captured, which is useful for foot placement [22]. We selected the instant following heel strike as the poincaré section for ankle control because this minimized time between sampling of the state and implementing changes in ankle push-off.

D. Controller performance comparison

After testing the model's stability without step-to-step control, we examined the control authority of each of the six actuation parameters to understand their effect on each state. The actuation parameters were: 1) step-length modulation, ϕ_{hf}, 2) step-width modulation, ϕ_{ha}, 3) proportional gain of the ankle inversion/eversion torque, Kp, 4) derivative gain of the ankle inversion/eversion torque, Kd, 5) ankle plantar-flexion stiffness, K, and 6) ankle push-off torque offset, τ_p. We then compared the ability of the step-to-step parameter modulation to recover from a disturbance during walking. We measured maximum allowable disturbance height while the model walked 500 steps on uneven ground. We also tested the

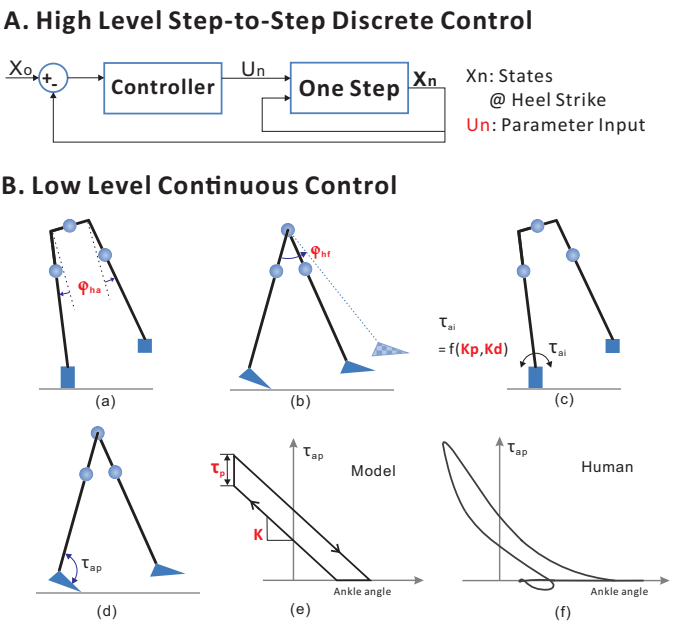

Fig. 5. Two layers of control. At the beginning of each step, the high level controller modulated actuation parameters (shown in red) for low level controllers. The low level controller performs continuous hip and ankle control during stance. (a) Step width was modulated by changing hip ab/aduction angle, ϕ_{ha}. (b) Step length was adjusted by controlling hip flex/extension angle, ϕ_{hf}. (c) Ankle inversion/eversion resistance torque was controlled by proportional, Kp, and damping, Kd, gains. (d) Ankle planatarflex torque, τ_{ap} was calculated as (e) a function of joint angle and the sign of joint velocity, creating a work loop. Push-off parameters were torque offset, τ_p, and stiffness, K. (f) The normal torque-angle curve is provided for reference.

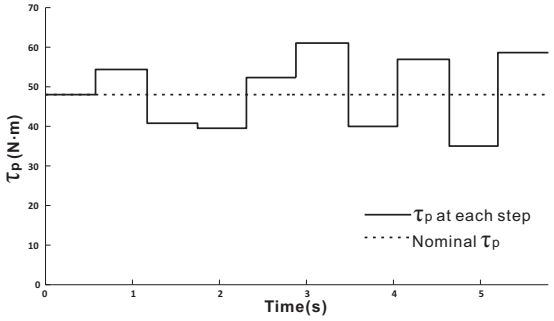

Fig. 6. Ankle torque offset at each of 10 steps during walking on uneven terrain. At the beginning of each step, the high level controller calculated a desired torque offset intended to attract the walking motion to the limit cycle. Then, the model took another step while following an ankle torque curve with the desired torque offset. The solid line is the desired torque offset and the dashed line is the nominal torque offset.

performance of a controller that combined all of these inputs.

III. RESULTS

With nominal actuation, we found a limit cycle at a speed of 1.25m/s and a step length of 0.7m. Without controlling nominal ankle and hip actuation parameters, the limit cycle was unstable, primarily in side-to-side motions as was found in previous studies [4, 23]. The step-to-step parameter control stabilized the model's walking with a wide range of maximum tolerable disturbances. Fig. 6 shows one example of step-to-step parameter modulation while the model walked on uneven terrain.

Ankle push-off modulation (τ_p), inversion resistance control (K_p,K_d), and step- width adjustment (ϕ_{ha}) had high control authority in side-to-side motion (Table I). Increase in ankle torque offset caused increasing forward and lateral direction velocity. Ankle inversion resistance control mostly affected side-to-side motion. Step length modulation (ϕ_{hf}) and ankle stiffness control (K) largely influenced fore-aft movement. We compared all of the control authorities at the poincareé section of following heel strike because at mid-stance, hip flexion angle was mostly affected by any parameter change.

Step-to-step ankle push-off parameter control effectively recovered the model from a maximum random floor height change of 3.2 cm (Fig. 7). The model successfully walked with lateral stabilization methods, such as step-width modulation and ankle roll resistance modulation similar to other studies ([4, 6]). The maximum random height tolerated was 1.2 cm (ϕ_{ha}), 1.1 cm (K_p), and 1.0 cm (K_d). Ankle stiffness modulation and step length modulation allowed the model to walk with disturbances of 0.2 cm and 0.02 cm, respectively.

IV. DISCUSSION

We hypothesized that ankle actuation might improve disturbance recovery during three dimensional walking. We found that step-to-step ankle push-off work control enhanced stability compared to other lateral stabilization methods such as step width modulation and ankle inversion resistance adjustment. The comparison with developed step-width modulation and ankle control seems to be reasonable considering the results of other foot stepping and zero moment point control studies. A study using the foot stepping strategy showed that a model, optimized for even ground walking with 65 cm step length, walked on 3 degree slope with 3.4 cm floor height changes [5]. Using ankle control paper, we estimated that continuous ankle control recovered a simulation model from a 2.5 cm ground height disturbance [6]. Since no studies used the same stability metric, we tested the maximum downward slope, our model could tolerate for 10 steps, for the purpose of comparison. With step-width modulation, the model walked down 3.1 cm (-2.5 deg) at each step, and with ankle roll resistance control the model walked down 5.7 cm (-4.7 deg). Hence, we think that we implemented a reasonable lateral stabilization controller.

TABLE I
NORMALIZED CONTROL AUTHORITY

		Control Input					
		ϕ_{hf}	ϕ_{ha}	Kp	Kd	K	τ_p
State	q_{tp}	-0.050	-0.041	-0.052	-0.029	0.075	0.117
	q_{ap}	-0.003	0.037	0.003	0.000	-0.056	-0.152
	q_{ai}	-0.005	-0.048	0.247	0.151	-0.031	0.119
	q_{hf}	0.088	-0.008	-0.026	-0.017	0.010	0.082
	$\dot{q}_{tp}$	-0.679	-0.472	0.028	0.179	0.755	-0.620
	$\dot{q}_{ap}$	0.718	0.594	-0.228	-0.343	-0.633	0.396
	$\dot{q}_{ai}$	-0.037	-0.643	0.939	0.909	-0.084	0.634
	$\dot{q}_{hf}$	-0.107	-0.076	-0.021	0.011	0.120	0.001

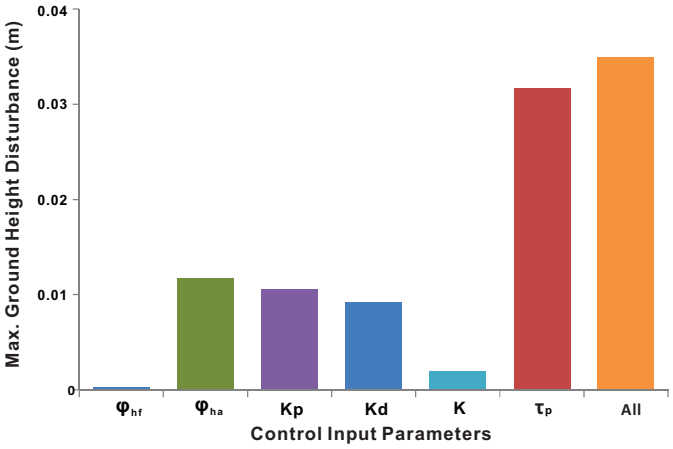

Fig. 7. Maximum bounded, random ground height variation the model could tolerate for 500 steps without falling. Six high-level control approaches were tested, with each modulating a separate parameter: step length, ϕ_{hf}; step width, ϕ_{ha}; ankle inversion stiffness, K_p; ankle inversion damping, K_d; ankle plantar-flexion stiffness, K; or ankle push-off torque offset, τ_p. Finally, a controller incorporating all inputs was evaluated. Surprisingly, ankle push-off work modulation enabled the model to overcome the largest disturbances, about three times as large as with lateral foot placement alone.

Compared to the lateral stabilization method, the step-to-step ankle push-off modulation seems an effective control method.

To understand the disturbance rejection ability of different step-to-step controllers, we looked at control authority. The push-off modulation had high control authority in the lateral direction as well as the fore-aft direction. The random ground disturbed the model in both directions; thus, the high control authority in both directions might have been helpful in disturbance recovery. Ankle inversion resistance control and step-width modulation may have been less able to reject disturbance, because they had dominant control authority in the lateral direction.

Our results have several limitations related to controller design and actuation pathways. We used a specific controller applicable to a linear region. Other controllers, such as such as LQR trees [24], might expand the disturbance rejection ability to further explore control capabilities. We also developed a simplified model of human motion and may have missed important human dynamics. For example, upper body actuation might be helpful for balance. However, our simulation with different low-level controllers and model parameters showed that step-to-step ankle control was effective when compared to the lateral foot stepping strategy. We tested disturbance rejection abilities using various nominal low-level hip controls and ankle controls including actuation with different ankle stiff nesses, proportional and derivate control of ankle resistance, and proportional and derivative control of step length. In addition, we experimented with different nominal step-widths and trunk inertias. Regardless of the different low-level controllers and nominal parameters, we found a similar overall trend: the maximum allowable disturbance ratio of ankle push-off modulation to step-width or ankle inversion/eversion resistance modulation was greater than two.

Our results show that step-to-step ankle push-off modulation is important for rejecting small disturbances. We further found that the ankle angles and angular velocities along with the step time were capable of generating the ankle push-off control input of the high-level controller. Hence, it would be relatively easy to implement in an active prosthesis.

V. CONCLUSION

In this study, we explored a three-dimensional models ankle and hip actuation capabilities of recovering from random ground height disturbances while walking. We found that most effective method to be ankle push-off modulation on a step-by-step basis. The performance improved with step-by-step step width modulation and ankle inversion resistance control. Although these results are limited to a specific controller and disturbance, they suggest that robotic ankle-foot prostheses could help individuals with below knee amputation to maintain their balance while walking. Implementing these strategies in hardware presents several challenges, including accurate sensing of human and prosthesis state in the ground reference frame. Addressing such challenges is left for future work.

[1] W. C. Miller, M. Speechley, and B. Deathe, "The prevalence and risk factors of falling and fear of falling among lower extremity amputees," *Arch. Phys. Med. Rehab.*, vol. 82, pp. 1031–1037, 2001.

[2] H. M. Herr and A. M. Grabowski, "Bionic ankle-foot prosthesis normalizes walking gait for persons with leg amputation," *Proc. Roy. Soc. Lon. B*, vol. 279, pp. 457–464, 2012.

[3] J. M. Donelan, R. Kram, and A. D. Kuo, "Mechanical and metabolic determinants of the preferred step width in human walking." *Proc. Roy. Soc. Lon. B*, vol. 268, pp. 1985–1992, 2001.

[4] A. D. Kuo, "Stabilization of lateral motion in passive dynamic walking," *Int. J. Rob. Res.*, vol. 18, pp. 917–930, 1999.

[5] J. M. Wang, D. J. Fleet, and A. Hertzmann, "Optimizing walking controllersl," *ACM Transactions on Graphics*, vol. 28, p. Article 168, 2009.

[6] S. Kajta and K. Tani, "Study of dynamic biped locomotion on rugged terrain-derivation and application of the linear inverted pendulum mode," in *Proc. Int. Conf. Rob. Autom.*, 1991, pp. 1405–1411.

[7] K. Yokoi, "Experimental study of humanoid robot HRP-1S," *Int. J. Rob. Res.*, vol. 38, pp. 351–362, 2004.

[8] A. Ruina, J. E. A. Bertram, and M. Srinivasan, "A collision model of the energetic cost of support work qualitatively explains leg sequencing in walking and galloping, pseudo-elastic leg behavior in running and the walk-to-run transition," vol. 237, pp. 170–192, 2005.

[9] D. G. E. Hobbelen and M. Wisse, "Ankle actuation for limit cycle walkers," *Int. J. Rob. Res.*, vol. 27(6), pp. 709–735, 2008.

[10] P. Bhounsule, J. Cortell, and A. Ruina, "Cornell ranger: Implementing energy-optimal trajectory control using low information, reflex-based control," in *Proc. Dynamic Walking*, 2012.

[11] A. D. Kuo, J. M. Donelan, and A. Ruina, "Energetic consequences of walking like an inverted pendulum: step-to-step transitions," *Exerc. Sport Sci. Rev.*, vol. 33, pp. 88–97, 2005.

[12] M. M. van der Krogt *et al.*, "How crouch gait can dynamically induce stiff-knee gait," *Ann. Biomed. Eng.*, vol. 38(4), pp. 1593–1606, 2010.

[13] C. E. Bauby and A. D. Kuo, "Active control of lateral balance in human walking," *J. Biomech.*, vol. 33, pp. 1433–1440, 2000.

[14] S. M. O'Connor and A. D. Kuo, "Direction-dependent control of balance during walking and standing," *J. Neurophys.*, vol. 102, pp. 1411–1419, 2009.

[15] D. Hobbelen, T. de Boer, and M. Wisse, "System overview of bipedal robots flame and tulip: Tailor-made for limit cycle walking," in *Proc. Int. Conf. Intel. Rob. Sys.*, 2008, pp. 2486–2491.

[16] E. R. Westervelt *et al.*, *Feedback control of dynamic bipedal robot locomotion*. Boca Raton: CRC press, 2007.

[17] S. H. Collins *et al.*, "Efficient bipedal robots based on passive-dynamic walkers," *Science*, vol. 307, pp. 1082–1085, 2005.

[18] D. A. Winter, *The Biomechanics and Motor Control of Human Gait: Normal, Elderly and Pathological*. Waterloo: Waterloo Biomechanics, 1991.

[19] R. Chandler *et al.*, "Investigation of inertial properties of the human body," AIR FORCE AEROSPACE MEDICAL RESEARCH LAB WRIGHT-PATTERSON AFB OH, No. AMRL-TR-74-137, 1975.

[20] A. D. Kuo, "The dynamics workbench," 2012. [Online]. Available: http://www-personal.umich.edu/ artkuo/DynamicsWorkbench/

[21] M. Wisse *et al.*, "How to keep from falling forward; elementary swing leg action for passive dynamic walkers," *Trans. Rob.*, vol. 21, pp. 393–401, 2005.

[22] K. Yin, K. Loken, and M. van de Panne, "Simbicon: Simple biped locomotion control," *ACM Trans. Graph.*, vol. 26, p. Article 105, 2007.

[23] J. Adolfsson, H. Dankowicz, and A. Nordmark, "3d passive walkers: Finding periodic gaits in the presence of discontinuities," *Nonlinear Dynamics*, vol. 24(2), pp. 205–229, 2001.

[24] R. Tedrake *et al.*, "Lqr-trees: Feedback motion planning via sums-of-squares verification," *Int. J. Rob. Res.*, vol. 29, pp. 1038–1052, 2010.